Experimental Parasitology 205 (2019) 107753

Contents lists available at ScienceDirect

Experimental Parasitology

journal homepage: www.elsevier.com/locate/yexpr

Anti-parasitic dinuclear thiolato-bridged arene ruthenium complexes alter the mitochondrial ultrastructure and membrane potential in *Trypanosoma brucei* bloodstream forms

Jennifer Jelk[a], Vreni Balmer[b], David Stibal[c], Federico Giannini[d], Georg Süss-Fink[c], Peter Bütikofer[a,***], Julien Furrer[d,**], Andrew Hemphill[b,*]

[a] Institute of Biochemistry and Molecular Medicine, University of Bern, Bern, Switzerland
[b] Institute of Parasitology, Vetsuisse Faculty, University of Bern, Länggassstrasse 122, CH-3012 Berne, Switzerland
[c] Institut de Chimie, Université de Neuchâtel, Avenue de Bellevaux 51, CH-2000 Neuchâtel, Switzerland
[d] Department of Chemistry and Biochemistry, Freiestrasse 3 CH-3012 Bern, Switzerland

A B S T R A C T

Trypanosoma brucei causes human African trypanosomiasis and Nagana disease in cattle, imposing substantial medical and economic burden in sub-Saharan Africa. The current treatments have limitations, including the requirement for elaborated protocols, development of drug resistance, and they are prone to adverse side effects. *In vitro* screening of a library of 14 dinuclear-thiolato bridged arene ruthenium complexes, originally developed for treatment of cancer cells, resulted in the identification of 7 compounds with IC_{50} values ranging from 3 to 26 nM. Complex $[(\eta^6\text{-}p\text{-}MeC_6H_4Pr^i)_2Ru_2(\mu_2\text{-}SC_6H_4\text{-}o\text{-}Pr^i)_3]Cl$ **(2)** (IC_{50} = 4 nM) and complex $[(\eta^6\text{-}p\text{-}MeC_6H_4Pr^i)_2Ru_2(\mu_2\text{-}SCH_2C_6H_4\text{-}p\text{-}Bu^t)_2(\mu_2\text{-}SC_6H_4\text{-}p\text{-}OH)]BF_4$ **(9)** (IC_{50} = 26 nM) were chosen for further assessments. Application of complex **2** and **9** at 20 nM and 200 nM, respectively, for 4.5 h induced alterations in the trypanosome mitochondrion as evidenced by immunofluorescence employing an antibody against mitochondrial Hsp70 and Mitotracker labeling. Transmission electron microscopy of parasites taken at 2 and 4h of treatment demonstrated massive alterations in the mitochondrial ultrastructure, while other organelles and structural elements of the parasites remained unaffected. Complex **2** treated trypanosomes exhibited a distorted mitochondrial membrane, and the mitochondrial matrix was transformed into an amorphous mass with different degrees of electron densities. Complex **9** did not notably impair the integrity of the membrane, but the interior of the mitochondrion appeared either completely translucent, or was filled with filamentous structures of unknown nature. Dose- and time-dependent effects of these two compounds on the mitochondrial membrane potential were detected by tetramethylrhodamine ethyl ester assay. Thus, the mitochondrion and associated metabolic processes are an important target of dinuclear thiolato-bridged arene ruthenium complexes in *T. brucei.*

1. Introduction

Human African trypanosomiasis (HAT), also referred to as African sleeping sickness, is induced by infection with the flagellated protozoan parasites *Trypanosoma brucei gambiense* and *T. b. rhodesiense*. While *T. b. gambiense* is responsible for 98% of all HAT cases, causing chronic infection, and is found in Western and Central Africa, *T. b. rhodesiense* causes a rapidly progressive form of the disease, and is found in Eastern and Southern Africa (Franco et al., 2014). Another *T. brucei* subspecies, *T. b. brucei*, is one of the causative agents of a wasting disease in cattle, called Nagana, affecting agricultural production and animal husbandry and causing high economic and social impact in African rural areas (Giordani et al., 2016). The drugs in clinical use for the treatment of HAT include pentamidine and suramin for the early and peripheral stage of the disease, and melarsoprol and eflornithine alone or in combination with nifurtimox for the cerebral phase (Büscher et al., 2017). Novel drugs being evaluated in phase II/III clinical trials include oxaborole (SCYX-7158), a benzoxaborole, and the 2-5-nitroimidazole fexinidazole that has recently been approved for human use (www.dndi.org). Veterinary trypanocides to treat Nagana include diminazene aceturate and isometamidium chloride as the two most commonly used drugs (Holmes, 2013).

One of the characteristics of the trypanosomatids is that they harbor only one mitochondrion per cell, compared to mammalian cells, which typically possess hundreds of individual mitochondria. In addition, unlike most other eukaryotes, the trypanosome mitochondrion contains

* Corresponding author.
** Corresponding author.
*** Corresponding author.
E-mail addresses: peter.buetikofer@ibmm.unibe.ch (P. Bütikofer), julien.furrer@dcb.unibe.ch (J. Furrer), andrew.hemphill@vetsuisse.unibe.ch (A. Hemphill).
URLs: http://ibmmsrvlakitu.unibe.ch/Buetikofer/ (P. Bütikofer), https://furrer.dcb.unibe.ch/ (J. Furrer), http://www.ipa.vetsuisse.unibe.ch/ueber_uns/personen/prof_dr_hemphill_andrew/index_ger.html (A. Hemphill).

https://doi.org/10.1016/j.exppara.2019.107753
Received 25 June 2019; Received in revised form 20 August 2019; Accepted 25 August 2019
Available online 27 August 2019

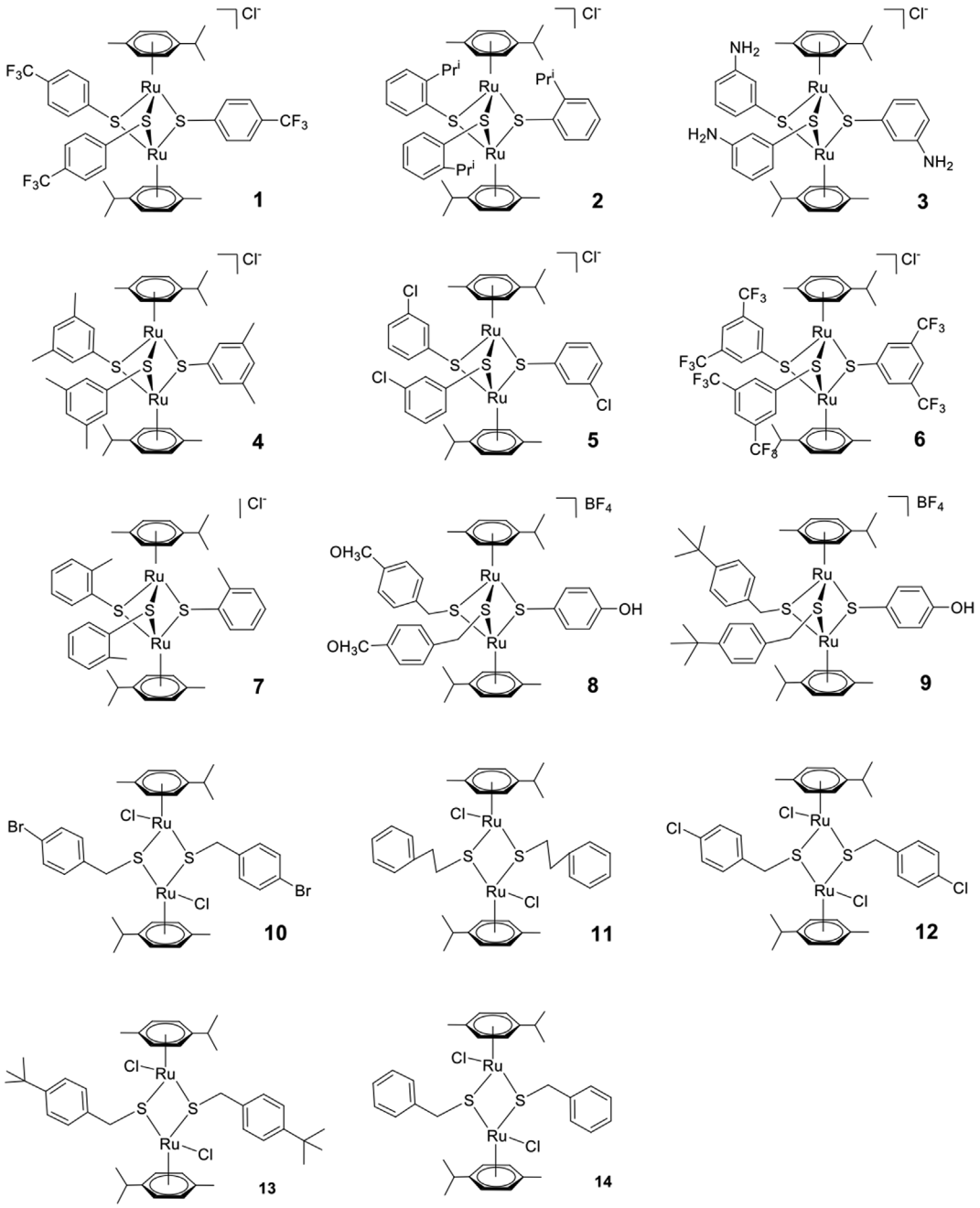

Fig. 1. Structures of the investigated dinuclear thiolato-bridged arene ruthenium complexes. (**1–7**) are cationic symmetrical trithiolato complexes bearing one type of thiol ligand, (**8–9**) are cationic mixed trithiolato complexes bearing two different thiol ligands, and (**10–14**) are neutral dithiolato complexes bearing one type of thiol ligand).

a single-unit mitochondrial genome, termed kinetoplast (Schneider and Oschsenreiter, 2018). The *T. brucei* life cycle alternates between the tsetse fly vector and a mammalian host. Mammalian bloodstream form trypanosomes rely almost entirely on glycolysis for energy production and lack oxidative phosphorylation (Priest and Hajduk, 1994). As revealed by fluorescence and transmission electron microscopy (TEM), the bloodstream form mitochondrion adopts a tube-like structure that stretches throughout the entire cell body and is largely devoid of cristae. The kinetoplast is located in a dilated area of the mitochondrion and is physically associated with the flagellar base and the flagellar pocket (Schneider and Oschsenreiter, 2018). Although the respiratory chain is not functional in *T. brucei* bloodstream forms, the mitochondrion is essential for parasite survival. Thus, compounds targeting mitochondrial function and structural integrity represent attractive drug candidates.

Metallodrugs are widely employed both for diagnosis and therapy of a wide range of diseases, and have been generated using platinum, copper, gold or ruthenium for the application in cancer but also for combating infectious diseases caused by bacteria Southam et al. (2017), helminths (Hess et al., 2015; Küster et al., 2012), and protozoan parasites. We have previously reported that several mononuclear and dinuclear thiolato-bridged ruthenium complexes exhibit promising *in vitro* activities against the intracellular apicomplexan parasites *Toxoplasma gondii* and *Neospora caninum* (Basto et al., 2017, 2019). They were shown to efficiently inhibit host cell invasion, had an IC_{50} in the low nanomolar range, low host cell toxicity, and exposure of parasites to these compounds led to distinct alterations in the ultrastructure of the parasite mitochondrion.

Table 1
The efficacies (IC_{50}s) of dinuclear thiolate-bridged arene ruthenium complexes on *T. b. brucei* bloodstream forms, and for comparison, in human foreskin fibroblasts (HFF). [a]Chloride salts of the corresponding thiols of the complexes [**1**–**7**] and BF_4 salts for [**8** and **9**] were used for experiments. [b] data from Basto et al. (2017). [c] The log *P* values correspond to the values calculated for the thiol RSH groups. n, number of independent determinations. ND, not determined.

Complex[a]	T. b. brucei IC_{50} (nM)	n	HFF IC_{50} (μM)[b]	Log*P* (RSH)[c]	(RSH)
1	4.2 ± 1.2	2	800	3.49 ± 0.36	*4*-C_6H_4-CF_3
2	4.1 ± 1.3	5	> 1000	3.86 ± 0.28	*2*-C_6H_4–$CH(CH_3)_2$
4	29.3 ± 3.7	2	ND	3.44 ± 0.28	*3,5*-C_6H_3-$(CH_3)_2$
5	4.1	1	ND	3.10 ± 0.29	*3*-C_6H_4–Cl
6	3.2 ± 1.7	3	2.8	4.74 ± 0.47	*3,5*-C_6H_3-$(CF_3)_2$
7	9.0 ± 1.1	2	ND	2.98 ± 0.28	*2*-C_6H_4–CH_3
8	8.6	1	ND	2.20 ± 0.28	R1: CH_2-*4*-C_6H_4–OCH_3 R2: *4*-C_6H_4–OH
9	25.6 ± 4.7	5	5.1	3.38 ± 0.29	R1: CH_2-*4*-C_6H_4-$(CCH_3)_3$ R2: *4*-C_6H_4–OH

Organometallic complexes have been explored previously for the treatment of African trypanosomiasis (Ravera et al., 2018), but also for Chagas disease caused by *Trypanosoma cruzi* in South America, for which the current drugs do not satisfy the needs for safe and easy-to-use application procedures, and drug resistance is becoming a major problem (Southam et al., 2017). Previously designed compounds include Ru(II)–NO donor drugs that have potent activity against *T. cruzi in vitro* and in animal models, with one trans-[Ru(NO) $(NH_3)_4$imN]$(BF_4)_3$ compound exhibiting 10-fold higher anti-trypanosomal activity than others (Silva et al., 2009). A series of novel cis-[Ru(NO)$(bpy)_2$L]X_n] compounds were specifically designed to target *T. cruzi* glyceraldehyde 3-phosphate dehydrogenase, and when assessed against *T. cruzi* trypomastigotes, epimastigotes and amastigotes in Vero cells, respective compounds were 1000-fold more active against *T. cruzi* than benznidazole, the standard drug used for the treatment of Chagas disease (Silva et al., 2010). Anti-*T. cruzi* and anti-*T. brucei* activities were also demonstrated for Ru(II)-cyclopentadienyl complexes. Three complexes with the general structure [Ru(η_5-C_5H_5)(PPh_3)L] exhibited good selectivity indexes for *T. cruzi* (> 49) and *T. brucei* (> 6), with IC_{50} values in the micromolar range (Fernandez et al., 2015). These complexes interact with DNA and cause the generation of free radicals. A novel Ru (II)-cyclopentadienyl (Cp) clotrimazole (CTZ) complex [RuCp $(PPh_3)_2$(CTZ)](CF_3SO_3) was shown to be active against *T. cruzi* and *T. brucei*, and against several human tumor cell lines (Arce et al., 2015). This complex did not interact with DNA, but affected the conversion of sequalene to sequalene oxide in the sterol biosynthetic pathway in *T. cruzi* (Arce et al., 2015).

In this study, we investigated the *in vitro* activities of a small panel of 14 dinuclear thiolato-bridged arene ruthenium complexes against *T. brucei* bloodstream forms in culture.

2. Materials and methods

2.1. Chemicals and synthesis of ruthenium complexes

All reagents for chemical synthesis were commercially available. The synthesis of complexes **1**–**14** was reported previously (Basto et al., 2017, 2019). All complexes were isolated as chloride or tetrafluoroborate salts, were stable orange to red solids, and were dried in vacuum.

2.2. Culture of T. b. brucei bloodstream forms

T. b. brucei 427 bloodstream forms co-expressing T7 RNA polymerase and tetracycline repressor (Wirtz et al., 1999) were cultured in HMI-9 medium (Hesse et al., 1995) containing 10% heat-inactivated fetal bovine serum. Cultures were maintained under humidified conditions in 5% CO_2 at 37 °C.

2.3. In vitro drug screening and IC_{50} determination

Stock solutions of complexes (1 mM) were prepared in DMSO, heated or sonicated if necessary, and stored at room temperature. Each compound was tested at concentrations ranging from 250 nM to 0.1 nM (final concentrations in the assay). The concentration of DMSO in the assay was < 0.25% (v/v), i.e. a concentration at which parasite growth is not affected. The stability of the complexes in water/DMSO mixtures has been demonstrated previously (Basto et al., 2017, 2019). Screenings and IC_{50} calculations were done as follows: Assays were performed in 96-well flat-bottom plates, with each well containing 1.5×10^3 parasites in 100 μl culture medium with or without a serial drug dilution. Ten 2-fold drug dilutions were used. After 72 h of compound exposure, 10 μl AlamarBlue® (Resazurin; Sigma) was added to each well allowing a colour change via metabolic oxidation-reduction by viable trypanosomes during 2–3 h. Subsequently, plates were read with a Flexstation II microplate fluorimeter using an excitation wave length of 536 nm and an emission wave length of 588 nm. IC_{50} values were determined using the software GraphPad Prism 6. Inhibition of trypanosome growth by pentamidine was measured in each plate as internal positive control.

2.4. (Immuno-) Fluorescence microscopy

Staining of mitochondrial HSP70 (mtHSP70): Trypanosomes (5×10^6 cells/ml) cultured in 24-well flat-bottom plates for 4.5 h in the absence or presence of drugs (20 nM or 200 nM, final concentrations) were collected in Eppendorf tubes and washed once with phosphate-buffered saline (PBS; 137 mM NaCl, 2.7 mM KCl, 10 mM Na_2HPO_4, 1.76 mM KH_2PO_4, pH 7.4) and resuspended in PBS containing 1% (w/v) paraformaldehyde. After incubation for 3 min at room temperature, fixed parasites were washed with PBS before being allowed to adhere onto poly-l-lysine-coated slides (Sigma). After treatment with methanol for 5 min at −20 °C, parasite preparations were air-dried for 5 min at

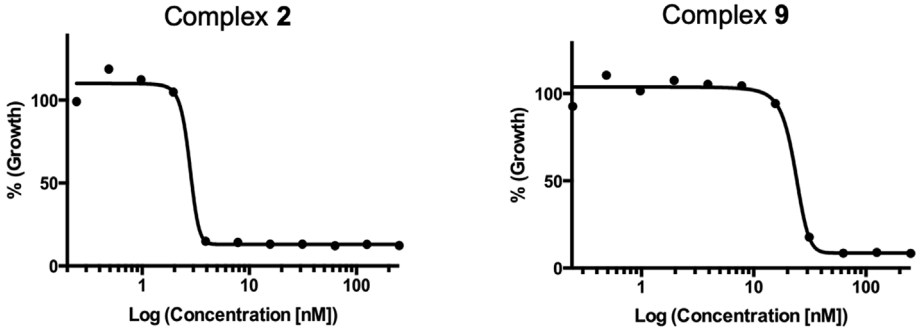

Fig. 2. Representative inhibition curves for complexes **2** and **9**.

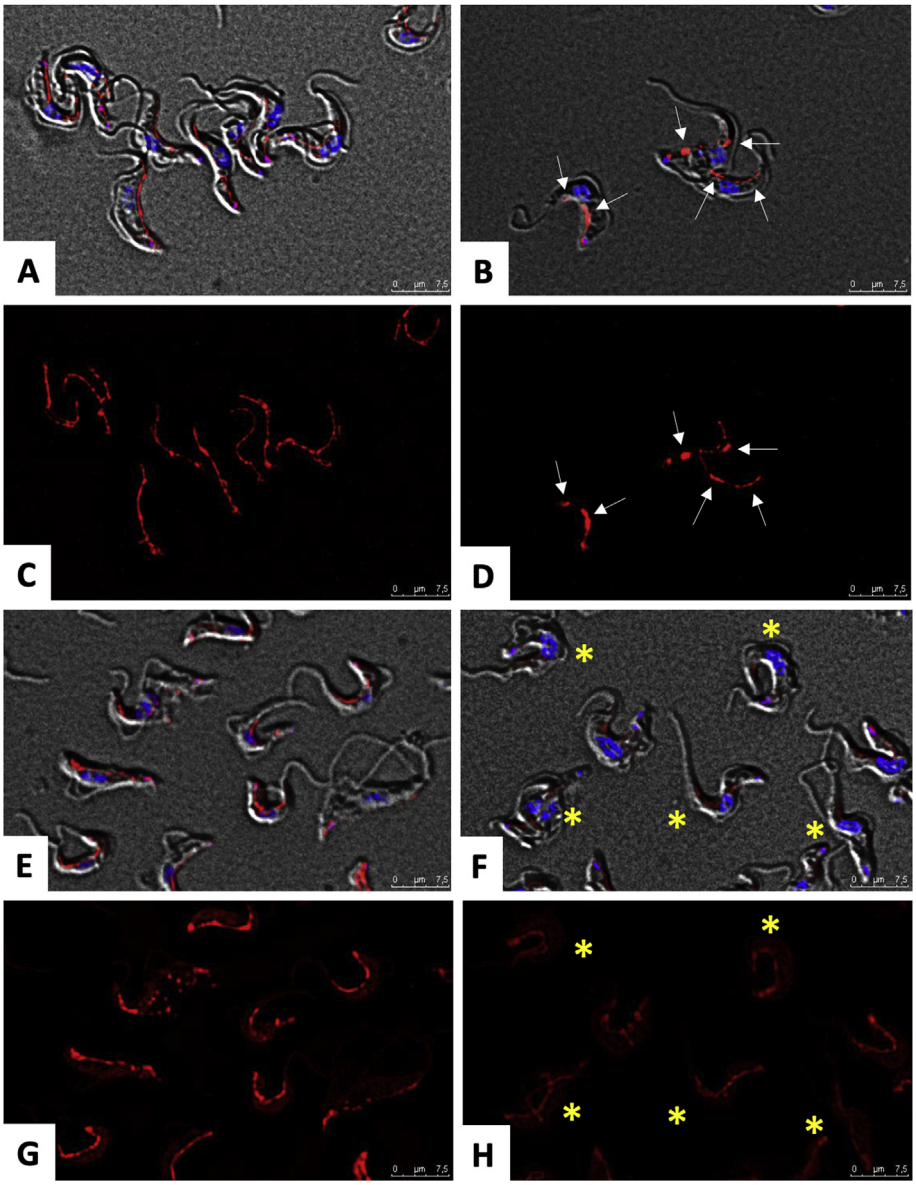

Fig. 3. Immunofluorescence staining of mtHSP70 and Mitotracker staining of *T. b. brucei* bloodstream forms treated with complex **2.** Anti-mtHSP70-labelled control trypanosomes are shown in A and C, trypanosomes exposed to 20 nM complex 2 during 4.5 h are depicted in B and D. Note a punctate staining pattern as indicated by arrows. Mitotracker staining of control parasites is shown in E and G, while complex 2-treated parasites are shown in F and H, with yellow asterisks indicating diminished labeling intensity. (For interpretation of the references to colour in this figure legend, the reader is referred to the Web version of this article.)

room temperature, humidified with PBS for 5 min and permeabilized with PBS containing 0.2% (w/v) Triton X-100 for 5 min. After blocking unspecific binding with PBS containing 2% (w/v) bovine serum albumin (blocking solution) for 30 min, parasites were exposed for 45 min to mouse α-mtHSP70 antibody (kindly provided by Paul Englund, Baltimore) at a dilution of 1:500 in blocking solution. After washing with PBS, goat α-mouse AlexaFluor 594 antibody (Invitrogen) at dilution of 1:1000 in blocking solution was added for 45 min. After washing and airdrying, cells were mounted with Vectashield containing DAPI. Fluorescence microscopy was performed with a Leica DMI6000 B inverted microscope using a 63x oil objective. Pictures were acquired, processed and 3D-deconvolved with Leica LAS AF Version 2.1.0 software (Leica Microsystems CMS GmbH).

Mitotracker staining: Trypanosomes (5×10^6 cells/ml) cultured in 24-well flat-bottom plates for 4 h in the absence or presence of drugs were exposed to MitoTracker™ Red CMXRos (Thermo Fisher Scientific; 0.1 μM in PBS) for 30 min. Parasites were then collected in Eppendorf tubes and washed with PBS containing 1% (w/v) paraformaldehyde. After incubation for 3 min at room temperature, cells were washed with PBS before being allowed to adhere onto poly-l-lysine-coated slides and air-dry for 5 min. Methanol treatment, air-drying, mounting on glass and examination by fluorescence microscopy was done as described above.

2.5. Transmission electron microscopy

Parasites exposed to drugs and control cultures during 2 or 4 h were washed in cold 100 mM sodium cacodylate buffer (pH 7.2) and re-suspended in the same buffer containing 2.5% (v/v) glutaraldehyde. Cells were fixed for 2 h at room temperature, followed by post-fixation in 2% OsO_4 in cacodylate buffer (pH 7.3). After three washes in distilled water, samples were pre-stained in Uranyless solution (Electron Microscopy Sciences, Hatfield, PA, USA) in distilled water for 20 min at room temperature and extensively washed in distilled water. Dehydration was carried out by stepwise incubation in ethanol (30%-50%-70%-90%–100%). Parasites were then embedded in EPON812

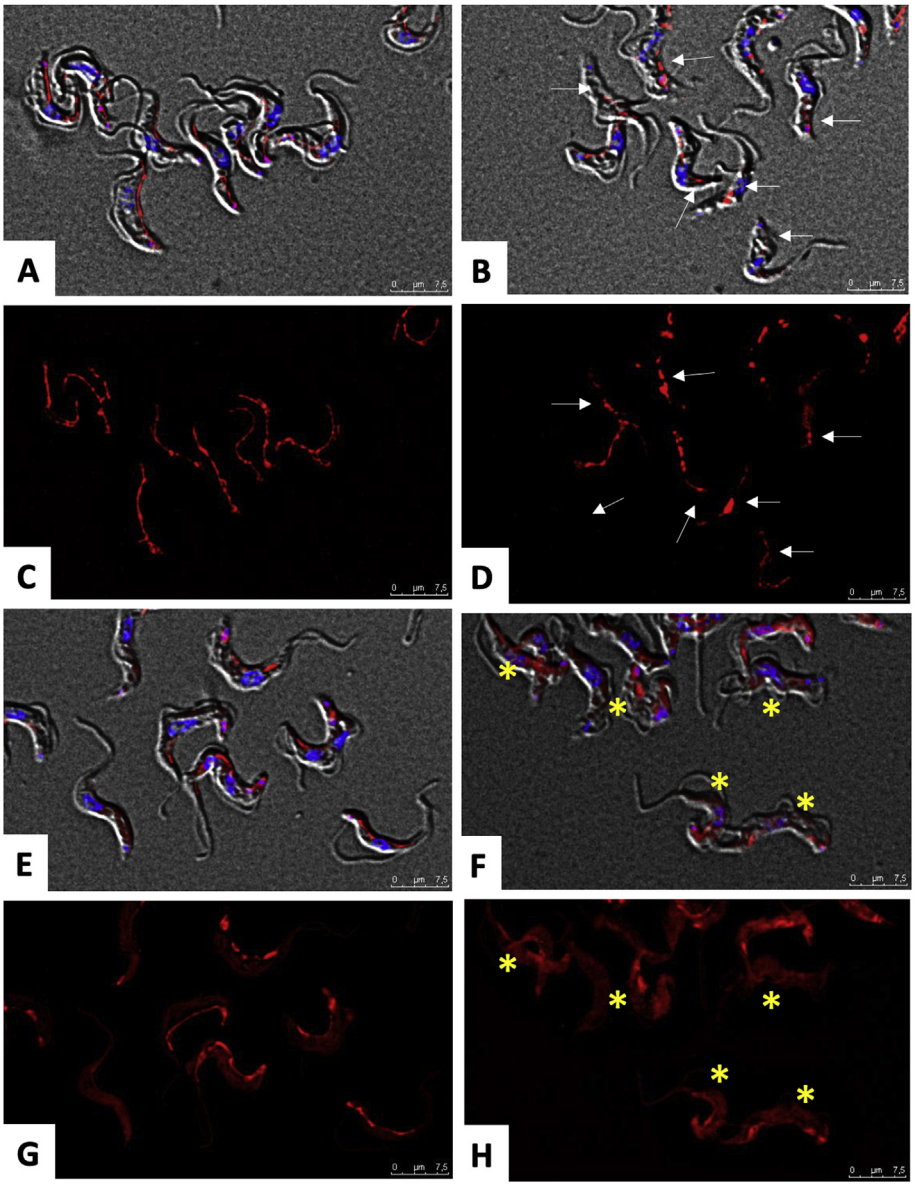

Fig. 4. Immunofluorescence staining of mtHSP70 and Mitotracker staining of *T. b. brucei* bloodstream forms treated with complex **9.** Anti-mtHSP70-labelled control trypanosomes are shown in A and C, trypanosomes exposed to 200 nM complex **9** during 4.5 h are depicted in B and D. Note a more punctate staining pattern as indicated by arrows. Mitotracker staining of control parasites is shown in E and G, while complex 9-treated parasites are shown in F and H, with yellow asterisks indicating slightly diminished labeling intensity. (For interpretation of the references to colour in this figure legend, the reader is referred to the Web version of this article.)

resin as described previously (Basto et al., 2017, 2019). Sections (80 nm) were cut on an ultramicrotome (Reichert & Jung, Vienna, Austria), placed onto 300-mesh formvar-carbon-coated nickel grids (Plano, Wetzlar, Germany), and sections were stained with Uranyless and lead citrate. Specimens were viewed on a CM12 transmission electron microscope operating at 60 kV.

2.6. Tetramethylrhodamine ethyl ester (TMRE) assay

Trypanosomes (5×10^6 cells/ml) cultured in 24-well flat-bottom plates for 2 h in the absence or presence of drugs were exposed for 30 min to TMRE (200 nM final concentration). Control trypanosomes were treated for 10 min with 25 μM carbonyl cyanide 3-chlorophenylhydrazone (CCCP; Sigma) to cause depolarization of the inner mitochondrial membrane. Parasites were then washed with PBS, resuspended in PBS and transferred to black 96-well flat-bottom plates, with each well containing 100 μl of sample. All samples were analyzed in triplicates. The plates were read with a TECAN Spark fluorescence plate reader, using an excitation wave length of 535 nm and an emission wave length of 595 nm. Quantification was done using the software GraphPad Prism 6. The values represent means ± standard deviations of triplicate determinations from 2 (complex 2) and 3 (complex 9) independent biological replicates. Statistical analysis was done by Kruskal-Wallis test, followed by Dunn's multiple comparison test. $P < 0.05$ indicated significant differences in TMRE signals in drug-treated parasites compared to the non-treated control.

3. Results

3.1. In vitro screening of dinuclear thiolato-bridged arene ruthenium complexes identifies several highly active compounds with anti-trypanosomal activity

A small library of 14 dinuclear thiolato-bridged arene ruthenium complexes (Fig. 1) was screened to search for compounds with *in vitro* activity against *T. b. brucei* bloodstream forms. This library encompasses 7 cationic trithiolato complexes $[(\eta^6\text{-}p\text{-}MeC_6H_4Pr^i)_2Ru_2(\mu_2\text{-}SC_6H_4\text{-}R)_3]Cl$ bearing one type of thiol ligand (**1–7**), 2 cationic mixed trithiolato complexes $[(\eta^6\text{-}p\text{-}MeC_6H_4Pr^i)_2Ru_2(\mu_2\text{-}SCH_2C_6H_4\text{-}R)_2(\mu_2\text{-}SC_6H_4\text{-}R)]BF_4$ bearing two different thiol ligands (**8–9**), and 5 neutral dithiolato complexes $[(\eta^6\text{-}p\text{-}MeC_6H_4Pr^i)_2Ru_2(\mu_2\text{-}SCH_2C_6H_4\text{-}p\text{-}R)_2Cl_2]$ bearing one type of thiol ligand (**10–14**). Each compound was tested for

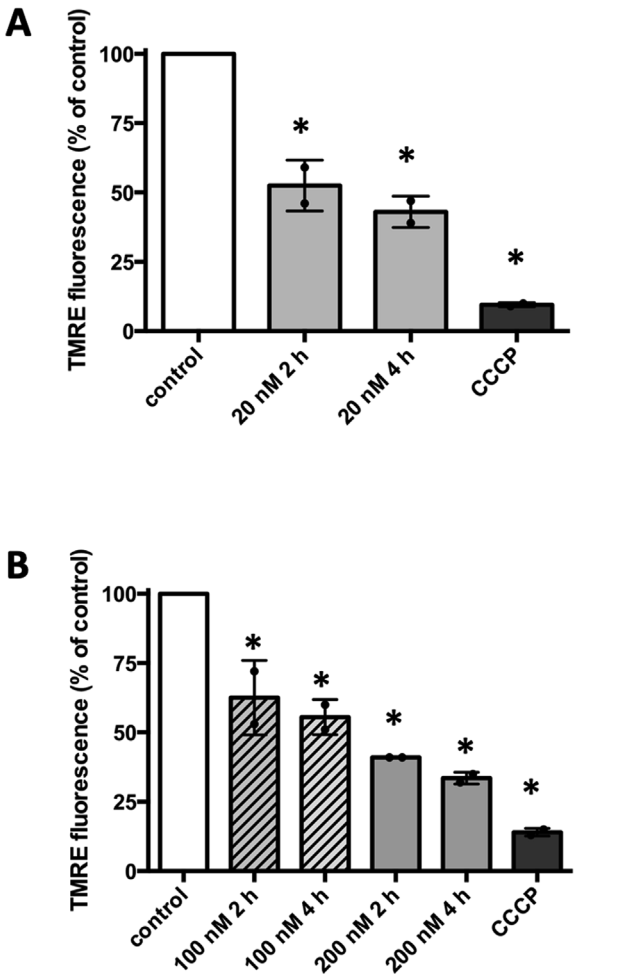

Fig. 5. Dose- and time-dependent impairment of the mitochondrial membrane potential as measured by TMRE uptake. Trypanosomes were exposed to 20 nM complex 2 during 2 or 4 h, or to 100 or 200 nM complex 9 during 2 and 4 h, respectively. The uncoupler CCCP was used as a positive control. The bars indicate the mitochondrial membrane potential in drug-treated trypanosomes relative to control untreated parasites. The values represent means ± standard deviations of triplicate determinations from 2 (complex 2) and 3 (complex 9) independent biological replicates. Statistical analysis was done by Kruskal-Wallis test, followed by Dunn's multiple comparison test to compare pair-by-pair. * indicates statistically significant differences ($P < 0.05$) in TMRE signals in drug-treated parasites compared to the non-treated control.

impairment of *T. b. brucei* bloodstream form viability between 250 nM and 0.1 nM (final concentrations in the assay). For 7 compounds, the IC_{50} values were > 100 nM and, thus, the compounds were no longer included in further analyses. In contrast, complexes **1**, **2** and **4**–**9** exhibited strong viability impairment. Their respective IC_{50} values are depicted in Table 1, and presented in relation to their log*P* in Fig. 2A. Six complexes had IC_{50} values between 3 and 10 nM (complexes **1**, **2**, **5**–**8**), while the IC_{50} values of complexes **4** and **9** were around 30 nM. Cytotoxicity of these complexes for human foreskin fibroblasts (HFF) monolayers was very low. Selective toxicity indexes (trypanosomes versus HFF) for complexes **1** and **2** were > 250′000. For compounds **6** and **9,** the respective IC_{50} values in HFF were 2.8 and 5.1 μM, i.e. approximately 930 and 215 times higher than for trypanosomes, respectively. Complexes **2** and **9**, with their respective inhibition curves shown in Fig. 2B, were studied in more detail.

3.2. Complexes 2 and 9 affect the mitochondrion

Previous investigations in the intracellular apicomplexan parasites *T. gondii* and *N. caninum* showed that ruthenium complexes primarily affected the ultrastructure of the parasite mitochondrion [10, 11]. To study potential mitochondrial alterations induced by these drugs in *T. b. brucei*, parasites were exposed to complex **2** (20 nM, ~5 x IC_{50}) and complex **9** (200 nM, ~8 x IC_{50}) during 4.5 h, and trypanosomes were stained by immunofluorescence using antibodies directed against the mitochondrial marker protein mtHSP70, or with Mitotracker, a fluorescent dye that incorporates into mitochondria only when the membrane potential is intact [19],

In control untreated trypanosomes, anti-mtHSP70 stained the entire length of the mitochondrion (Fig. 3A, C and 4A, C). In contrast, treatment parasites with 20 nM complex **2** resulted in a more punctated mitochondrial staining (Fig. 3B, D), and a similar staining pattern, although a bit less pronounced, was observed after a 4.5 h treatment with 200 nM complex **9** (Fig. 4B, D). Mitotracker staining of complex **2**-treated parasites resulted in diminished labeling, suggesting a drug-induced decrease in mitochondrial membrane potential (Fig. 3E–H). A similar effect on Mitotracker staining was also seen after exposure of parasites to complex **9**, although the loss in staining intensity was less evident (Fig. 4E–H). Further evidence for drug-dependent loss of mitochondrial membrane potential was obtained using TMRE as indicator (Fig. 5). TMRE signals were clearly diminished upon exposure of parasites to complexes **2** or **9** in a time- and concentration-dependent manner.

3.3. Detection of drug-induced mitochondrial damage by TEM

T. b. brucei bloodstream forms were exposed to 20 nM complex **2**, 200 nM complex **9**, or the corresponding vehicle during 2 and 4 h, and were fixed and processed for TEM. Sections of non-treated and vehicle-treated trypanosomes revealed the typical ultrastructural features of *T. b. brucei*, including a flagellum and a cell body with a nucleus containing an electron dense nucleolus, and the mitochondrion of which different parts were visible within the entire cytoplasm as more electron dense vesiculated entities on a single section (Fig. 6A). Higher magnification views exposed subpellicular microtubules that form the cytoskeleton of African trypanosomes, the Golgi-apparatus, the flagellar pocket, representing the site where the flagellum emerges from the cell body and runs along the longitudinal axis of the parasite, and the kinetoplast composed of mitochondrial DNA, closely associated with flagellum and flagellar pocket. While the mitochondrial matrix appears electron dense, only few cristae-like structures are visible in bloodstream form trypanosomes. After exposure of *T. b. brucei* bloodstream forms to complex **2** for 2 h (Fig. 7A and B) or 4 h (7C, D), the following structural alterations were observed: The mitochondrial membrane appeared distorted and poorly visible in some areas, and the mitochondrial matrix had lost its electron dense texture and appeared as amorphous, undefined area (Fig. 7A–D). In addition, mitochondrial swelling was observed, with the organelle occupying a larger part of the cytoplasm compared to non-treated cells. This was also the case for the region surrounding the kinetoplast at both time points (Fig. 7E and F). In contrast, other organelles of the parasite, such as the Golgi apparatus, did not appear to be structurally affected after exposure to complex **2.**

Complex **9**, applied at 200 nM, also affected the ultrastructure of the mitochondrion, but the effects were different compared to complex **2**-treated parasites (Fig. 8A–D). The mitochondrial membrane was structurally mostly intact, and the matrix in complex **9**-treated trypanosomes was not filled with an amorphous substance, but with filamentous material of unknown composition. As for complex **2**, other organelles including the cytoskeleton, flagellar pocket and the Golgi-apparatus remained largely unaffected by treatment with complex **9**.

4. Discussion

We here report on promising *in vitro* activities of a panel of

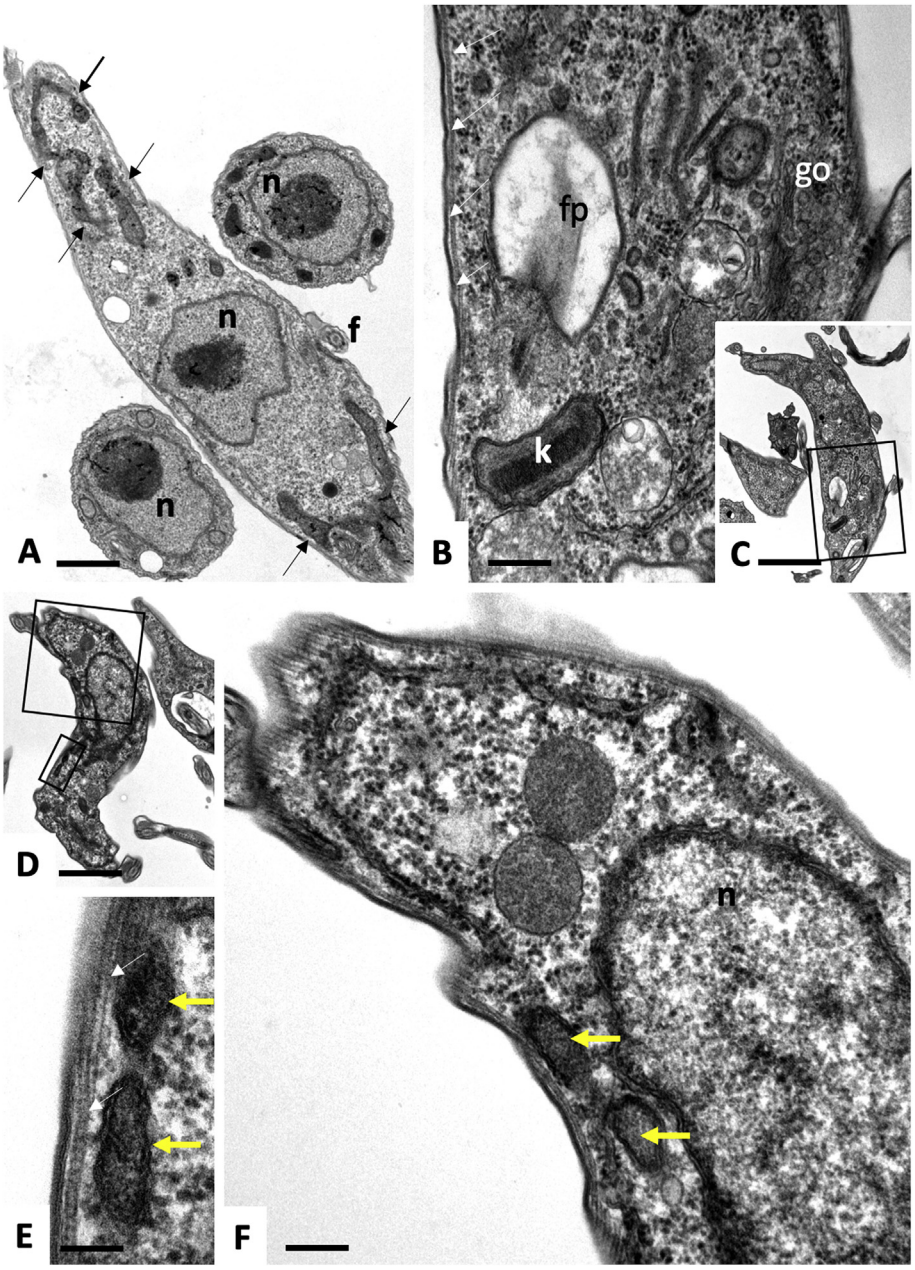

Fig. 6. Ultrastructure of control (A) and vehicle (B–F)-treated *T. b. brucei* visualized by TEM. A is a low magnification view of one longitudinal and two cross-sections; n = nucleus; black arrows point towards portions of the mitochondrion seen in a single section. B is a higher magnification view of the boxed area of the parasite seen in C; fp indicates the flagellar packet, k = kinetoplast, go = Golgi stacks. E and F are higher magnification views of the boxed areas shown in D. Yellow arrows point towards the mitochondrion, the white arrow in E shows subpellicular microtubules. Bars in A = 0.4 µm; B = 0.17 µm; C = 1.2 µm; D = 1.2 µm; E and F = 0.17 µm. (For interpretation of the references to colour in this figure legend, the reader is referred to the Web version of this article.)

dinuclear thiolate-bridged arene ruthenium complexes against *T. b. brucei* bloodstream forms. Of 14 compounds that were initially tested at 250 nM, seven exhibited severe impairment of parasite viability. Six compounds (**1, 2, 5–8**) had IC_{50} values below 10 nM, and two (4, **9**) exhibited IC_{50} values of around 30 nM.

In line with previous studies showing that complexes **10–14** were only moderately cytotoxic *in vitro* against several cancer cell lines (IC_{50} values between 0.2 and 2.5 µM) (Ibao et al., 2012; Stibal et al., 2014) and not toxic against *T. gondii* and *N. caninum*, they were also not affecting the viability of *T. b. brucei* bloodstream forms. This may reflect their propensity to easily get hydrolysed compared to their trithiolato counterparts (Basto et al., 2017, 2019).

Generally, the *in vitro* activity of anticancer and antiparasitic drugs can be related in part to their lipophilic character. In general, increasing hydrophobicity facilitates uptake of a compound by cells or parasites, thereby enhancing its anti-proliferative activity. We and others have previously demonstrated correlation between lipophilicity and cytotoxic activity for dinuclear arene ruthenium complexes, e.g. in studies involving the apicomplexan parasites *T. gondii* and *N. caninum* (Basto et al., 2017, 2019). Complexes with log *P* values in the range between 3.0 and 4.0 showed highest cytotoxicity, whereas complexes with log *P* values lower than 3.0 or higher than 4.5 were less active, presumably due to poor cellular uptake. Generally, less lipophilic compounds have more difficulties to cross membranes or are more rapidly excreted by exocytosis. Interestingly, as shown in Table 1, the activity of this library of arene ruthenium complexes against *T. b. brucei* does not mirror our findings obtained earlier in several cancer cells (Giannini et al., 2012, 2013) and in the apicomplexan parasites *Toxoplasma gondii* and *N. caninum*. There is indeed only a poor correlation between lipophilicity and IC_{50} values: for instance, complex **1** has a log *P* value of 3.48 and an IC_{50} value of 3 nM, while complex **4** has a similar log *P* value of 3.44 but is non-toxic. Similarly, complexes **1**, **2**, and **5–8** exhibit similar IC_{50} values between 3 and 9 nM, while their log *P* values range from 2.20 (**8**, hydrophilic) to 4.74 (**6**, very lipophilic).

The character of the substituents in the thiolato-ligands seems to play an important role in the differences in anti-trypanosomal activity,

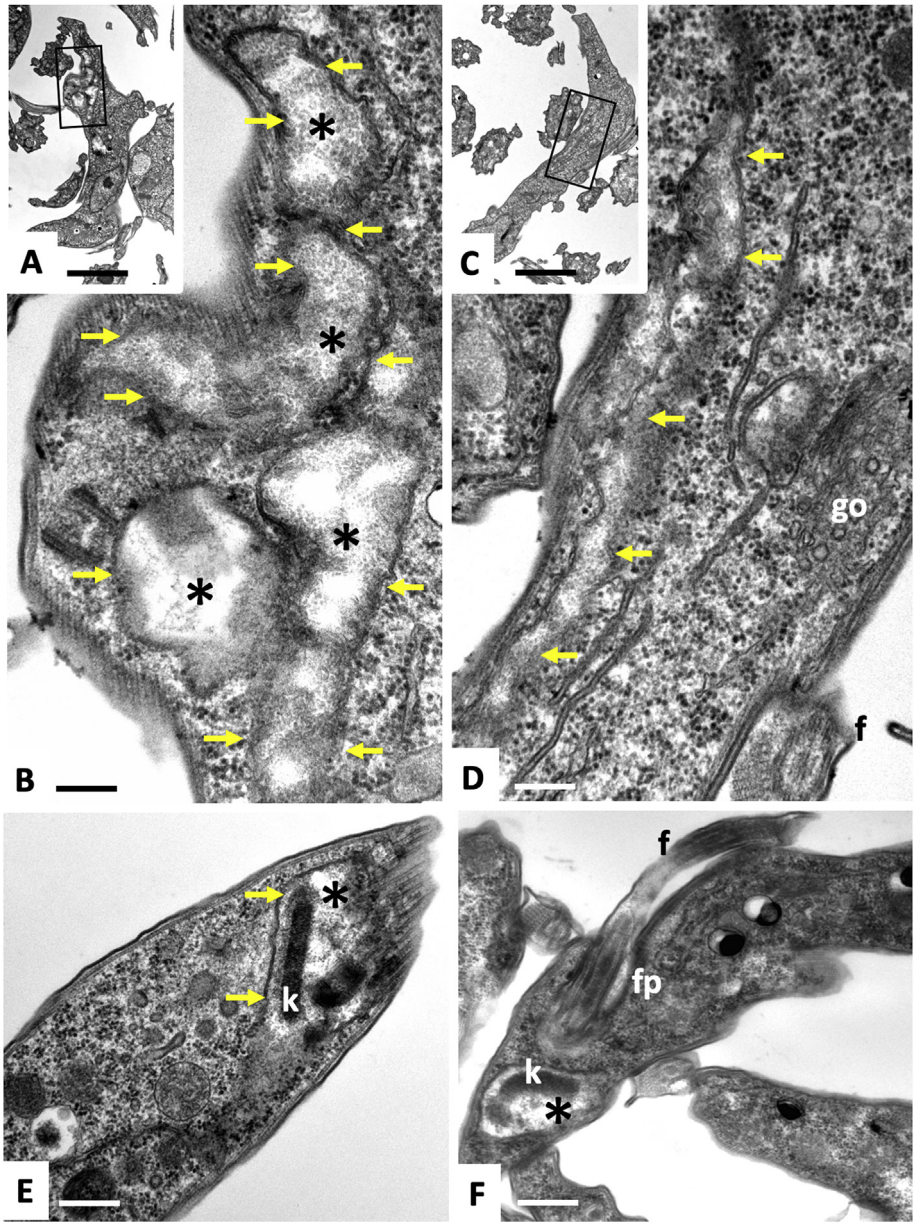

Fig. 7. TEM carried out after exposure of *T. b. brucei* to 20 nM complex **2** during 2 h (A, B) or 4 h (E, F). The boxed areas in A and C are magnified in B and D, respectively. The mitochondrial membrane is indicated by yellow arrows, and the * indicates the less electron dense mitochondrial matrix. E and F show regions around the flagellar pocket (fp), with the kinetoplast (k), and a rather amorphous and electron-lucent matrix (*). Bars in A = 1.2 μm; B = 0.12 μm; C = 1.2 μm; D = 0.12 μm; E = 0.22 μm; F = 0.28 μm. (For interpretation of the references to colour in this figure legend, the reader is referred to the Web version of this article.)

whereas the position of the substituents in the thiolato-ligands seems to have little influence. Whatever the substituent position is, complexes with heteroatoms exhibit increasing IC_{50} values that parallel the lipophilicity of the corresponding thiol, going from **3** (R = 3-C_6H_4–NH_2) to **6** (R = 3,5-C_6H_3-$(CF_3)_2$). In contrast, complexes with aliphatic substituents such as complex **2** (R = 2-C_6H_4–$CH(CH_3)_2$), **4** (R = 3,5-C_6H_3-$(CH_3)_2$) and **7** (R = 2-C_6H_4–CH_3) exhibit IC_{50} values that do not correlate with lipophilicity.

Complexes **2** and **9** were further characterized, since the efficacy and the ultrastructural effects of these compounds have been also assessed previously against *T. gondii* and *N. caninum* (Basto et al., 2017, 2019). We here provide evidence that, within 2–4 h of exposure, these compounds induced severe ultrastructural changes such as mitochondrial swelling and dissolution of the cristae, the mitochondrial matrix and mitochondrial membrane, while other organelles were seemingly unaffected. However, the absence of ultrastructural evidence does not exclude effects on other aspects of physiology and metabolism, thus it is possible that these compounds also target other organelles.

In addition, exposure to complex **2** or **9** also reduced the mitochondrial membrane potential in a time- and concentration-dependent manner. Oxidative phosphorylation resulting in generation of ATP is the major function of mitochondria in eukaryotic cells. However, *T. b. brucei* bloodstream forms largely lack this activity (Priest and Hajduk, 1994), but mitochondria are involved in other crucial processes. These include cell division and cell cycle regulation, t-RNA- and protein-import and mitochondrial protein translation, alternative oxidase, acetate production for cytosolic and mitochondrial fatty acid biosynthesis, the glycine cleavage complex/thymidine biosynthesis, production of ergosterol-related sterols by a biosynthetic pathway similar to that operating in pathogenic fungi, maintenance of a proper mitochondrial membrane potential, amino acid metabolism and calcium homeostasis. Mitochondria are also involved in the steps leading to programmed cell

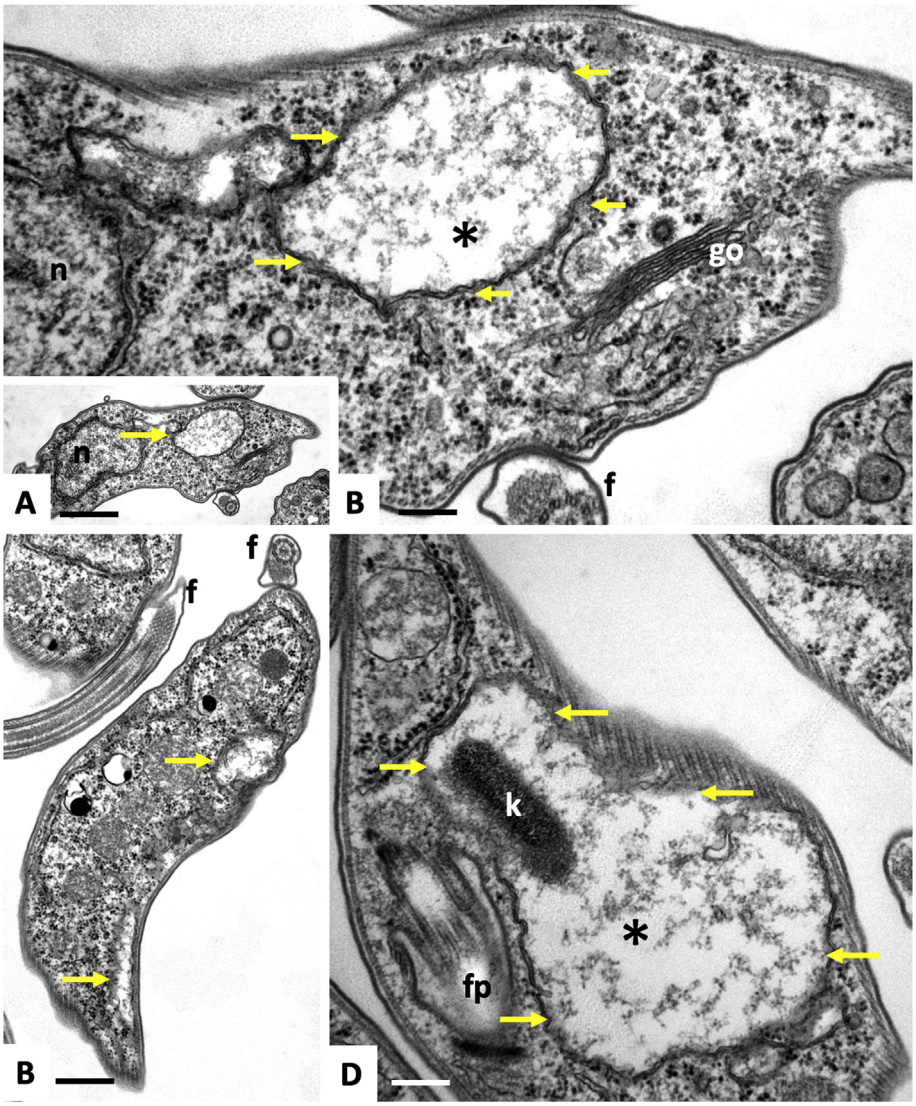

Fig. 8. TEM carried out after exposure of *T. b. brucei* to 200 nM complex **9** during 2 h (A, B) or 4 h (C, D). The section through the trypanosome in A is shown at higher magnification in B. Yellow arrows point towards the membranes of the mitochondrion, with a matrix (*) that has lost much of its electron dense content. D shows a flagellar pocket (fp) and the associated kinetoplast (k) surrounded by a swollen mitochondrion; go = Golgi. Bars in A = 0.7 μm; B = 0.15 μm; C = 0.35 μm; D = 0.15 μm. (For interpretation of the references to colour in this figure legend, the reader is referred to the Web version of this article.)

death (Fidalgo and Gille, 2011; Zimmer, 2019). In general, the most of the active complexes in our study are positively charged, whereas none of the neutral complexes were active. This implies that the positive charge could be an important factor in mitochondrial uptake of the complexes as the mitochondrial matrix is negatively charged.

A large panel of compounds has been shown previously to directly interfere with the mitochondrial ultrastructure in trypanosomatids, similar to the ruthenium compounds investigated here. Hentzer and Kobayasi (1977) demonstrated the effects of pentamidine on the mitochondria of *Leishmania tropica*, including mitochondrial swelling, disappearance of cristae, and changes in the kinetoplast. Similar alterations were reported in *T. brucei* after treatment with pentamidine, puromycin, acriflavine, antrycide, suramin and mapharside (Williamson et al., 1975). Membrane and cristae fragmentation and disruption of the kinetoplast core were also reported after treatment of *L. amazonensis* with pentamidine. However, changes in the kinetoplast also occur by abrupt disruption of the mitochondrial membrane potential and perturbation of Ca^{2+} homeostasis (Vercesi and Docampo, 1992), the former of which we demonstrate here after treatment with ruthenium complexes **2** and **9.**

Inhibitors of ergosterol and phospholipid biosynthesis were also shown to induce similar effects as seen with complexes **2** and **9**. Sterol methenyl transferase inhibitors dramatically affected the ultrastructure and physiology of the mitochondrion leading to potent growth inhibition of promastigotes of *L. amazonensis* (Rodrigues et al., 2007). The effects of ergosterol biosynthesis inhibitors have been explained by the large amounts of endogenous and exogenous sterols present in the mitochondrial membranes of e.g. *T. cruzi* (Rodrigues et al., 2001). Ergosterol biosynthesis inhibitors induce important alterations in the phospholipid content of the mitochondrial membranes, with an increase in phosphatidylethanolamine (PE) and a decrease in phosphatidylcholine (PC), probably due to inhibition of PE N-methyltransferase (Palmie-Peixoto et al., 2006). In the case of the phospholipid biosynthesis inhibitor miltefosine, studies in *Leishmania* sp. also demonstrated lesions in the mitochondrion, with subsequent DNA fragmentation, both characteristics of apoptosis-like cell death (Verma and Dey, 2004). Whether complex **2** and/or **9** interfere in lipid biosynthesis remains to be investigated. It would be surprising that the compounds 2 and 9 target these pathways, as their chemical structures are clearly different from the inhibitors of ergosterol and phospholipid biosynthesis.

In the intracellular apicomplexan parasite *T. gondii,* inhibitors of

ergosterol biosynthesis induced the most severe ultrastructural changes also in the mitochondrion, displaying intense swelling with a loss of matrix content (Martins-Duarte et al., 2006). Interestingly, this was also observed for complex **2** and **9** in *T. gondii* (Basto et al., 2017) and *N. caninum* (Basto et al., 2019). Affinity chromatography of *Toxoplasma* soluble extracts on epoxy-sepharose-bound complex **9** identified *T. gondii* translation elongation factor 1-alpha (Tg-EF1-alpha) and two ribosomal proteins, RPS18 and RPL27, as potential binding proteins (Basto et al., 2017). In eukaryotic cells, EF1-alpha is an essential component of protein synthesis, promoting the GTP-dependent transfer of aminoacylated tRNA to the ribosome A site. Other activities of EF1-alpha are associated with vital cellular functions related to cell growth, motility, protein metabolism, signal transduction, DNA replication/repair protein networks, and apoptosis (Toueille et al., 2007; Lamberti et al., 2007). In *T. gondii* and *T. brucei*, EF1-alpha mediates the specificity of mitochondrial tRNA import (Bouzaidi-Tiali et al., 2007; Esseiva et al., 2004), and disruption of this process could lead to the observed mitochondrial alterations. Involvement of EF1-alpha in the mechanism of action of complexes **2** and **9** should be investigated in further studies.

In conclusion, we demonstrate remarkable changes in the mitochondrion of bloodstream forms of *T. b. brucei* during short-term exposure to several ruthenium complexes. Corresponding IC_{50} values in trypanosomes are in the lower nanomolar range, and these complexes exhibit highly favorable selective toxicity indeces as they are not toxic for human fibroblasts. However, other mammalian cell types need to be studied ensure proper selective toxicity for protozoan parasites. Future investigations will focus on extensive structure-activity relationships by modifying the arene ligands and anchoring bioactive molecules, a strategy already explored by some of us for this family of complexes against cancer cells [24]. Furthermore, the functionalization of these arene ruthenium complexes with fluorescent molecules such as BODIPY or Coumarin derivatives will enable us to get more insights into their mechanism of action, most notably on how they impair the mitochondrion. Finally, we will examine whether they exert true parasiticidal activity.

Declararations of interest

None.

Funding

This work was financed through the National Science Foundation grants No. CRSII_173718 (JF&AH) and 31003A_169355(PB).

Conflicts of interest

No conflict of interest.

Ethical approval

Not required.

Acknowledgements

The authors wish to thank Afonso Basto, Joachim Müller and Norbert Müller for helpful discussions and many pieces of advice.

References

Arce, E.R., Sarniguet, C., Moraes, T.S., Vieites, M., Tomaz, A.I., Medeiros, A., Comin, M.A., Varela, J., Cerecetto, H., Gonzales, M., Marques, F., Garcia, M.H., Otero, L., Gambino, D., 2015. A new ruthenium cyclopentadienyl azole compound with activity on tumor cell lines and trypanosomatid parasites. J. Coord. Chem. 68, 2923–2937. https://doi.org/10.1080/00958972.2015.1062480.

Basto, A.P., Müller, J., Rubbiani, R., Stibal, D., Giannini, F., Süss-Fink, G., Balmer, V., Hemphill, A., Gasser, G., Furrer, J., 2017. Characterization of the activities of dinuclear thiolato-bridged arene ruthenium complexes against Toxoplasma gondii. Antimicrob. Agents Chemother. 61https://doi.org/10.1128/AAC.01031-17. e01031-17.

Basto, A.P., Anghel, N., Rubbiani, R., Müller, J., Stibal, D., Giannini, F., Süss-Fink, G., Balmer, V., Gasser, G., Furrer, J., Hemphill, A., 2019. Targeting of the mitochondrion by dinuclear thiolato-bridged arene ruthenium complexes in cancer cells and in the apicomplexan parasite *Neospora caninum*. Metallomics 11, 462–474. https://doi.org/10.1039/c8mt00307f.

Bouzaidi-Tiali, N., Aeby, E., Charrière, F., Pusnik, M., Schneider, A., 2007. Elongation factor 1a mediates the specificity of mitochondrial tRNA import in T. brucei. EMBO J. 26, 4302–4312.

Büscher, P., Cecchi, G., Jamonneau, V., Priotto, G., 2017. Human african trypanosomiasis. Lancet 390, 2397–2409. https://doi.org/10.1016/S0140-6736(17)31510-6.

Esseiva, A.C., Naguleswaran, A., Hemphill, A., Schneider, A., 2004. Mitochondrial tRNA import in Toxoplasma gondii. J. Biol. Chem. 279, 42363–42368.

Fernandez, M., Arce, E.R., Sarniguet, C., Morais, T.S., Tomaz, A.I., Azar, C.O., Figueroa, R., Diego Maja, J., Medeiros, A., Comini, M., Helena Garcia, M., Otero, L., Gambino, D., 2015. Novel ruthenium(II) cyclopentadienyl thiosemicarbazone compounds with antiproliferative activity on pathogenic trypanosomatid parasites. J. Inorg. Biochem. 153, 306–314. https://doi.org/10.1016/j.jinorgbio.2015.06.018.

Fidalgo, L.M., Gille, L., 2011. Mitochondria and trypanosomatids: targets and drugs. Pharm. Res. 28, 2758–2770. https://doi.org/10.1007/s11095-011-0586-3.

Franco, J.R., Simarro, P.P., Diarra, A., Jannin, J.G., 2014. Epidemiology of human African trypanosomiasis. Clin. Epidemiol. 6, 257–275. https://doi.org/10.2147/CLEP.S39728.

Giannini, F., Furrer, J., Ibao, A.F., Süss-Fink, G., Therrien, B., Zava, O., Baquie, M., Dyson, P.J., Stěpnička, P., 2012. Highly cytotoxic trithiophenolatodiruthenium complexes of the type [(η6-p MeC6H4Pri)2Ru2(SC6H4-p-X)3]+: synthesis, molecular structure, electrochemistry, cytotoxicity, and glutathione oxidation potential. J. Biol. Inorg. Chem. 17, 951–960. https://doi.org/10.1007/s00775-012-0911-2.

Giannini, F., Paul, L.E.H., Furer, J., Therrien, B., Süss-Fink, G., 2013. Highly cytotoxic diruthenium trithiolato complexes of the type (n(6-p-MeC6H4Pri)2Ru2(μ(2)-SR)(3)(+): synthesis, characterization, molecular structure and in vitro anticancer activity. New J. Chem. 37, 3503–3511. https://doi.org/10.1039/c3nj00476g.

Giordani, F., Morrison, L.J., Rowan, T.G., DE Koning, H.P., Barrett, M.P., 2016. The animal trypanosomiases and their chemotherapy: a review. Parasitology 143, 1862–1889. https://doi.org/10.1017/S0031182016001268.

Hentzer, B., Kobayasi, T., 1977. The ultrastructural changes of Leishmania tropica after treatment with pentamidine. Ann. Trop. Med. Parasitol. 71, 157–166. https://doi.org/10.1080/00034983.1977.11687174.

Hess, J., Keiser, J., Gasser, G., 2015. Toward organometallic antischistosomal drug candidates. Future Med. Chem. 7, 821–830. https://doi.org/10.4155/fmc.15.22.

Hesse, F., Selzer, P.M., Mühlstädt, K., Duszenko, M., 1995. A novel cultivation technique for long-term maintenance of bloodstream form trypanosomes in vitro. Mol. Biochem. Parasitol. 70, 157–166.

Holmes, P., 2013. Tsetse-transmitted trypanosomes–their biology, disease impact and control. J. Invertebr. Pathol. 112 (Suppl. l), S11–S14. https://doi.org/10.1016/j.jip.2012.07.014.

Ibao, A.-F., Gras, M., Therrien, B., Süss-Fink, G., Zava, O., Dyson, P.J., 2012. Thiolato-bridged arene ruthenium complexes: synthesis, molecular structure, reactivity, and anticancer activity of the dinuclear complexes [(arene)2Ru2(SR)2Cl2]. Eur. J. Inorg. Chem. 1531–1535. https://doi.org/10.1002/ejic.201101057.

Küster, T., Lense, N., Barna, F., Hemphill, A., Kindermann, M.K., Heinicke, J.W., Vock, C.A., 2012. A new promising application for highly cytotoxic metal compounds: n6-areneruthenium(II) phosphite complexes for the treatment of alveolar echinococcosis. J. Med. Chem. 55, 4178–4188. https://doi.org/10.1021/jm300291a.

Lamberti, A., Longo, O., Marra, M., Tagliaferri, P., Bismuto, E., Fiengo, A., Viscomi, C., Budillo, A., Rapp, U.R., Wang, E., Venuta, S., Abbruzzese, A., Arcari, P., Caraglia, M., 2007. C-Raf antagonizes apoptosis induced by IFN-[alpha] in human lung cancer cells by phosphorylation and increase of the intracellular content of elongation factor 1A. Cell Death Differ. 14, 952–962. https://doi.org/10.1038/sj.cdd.4402102.

Martins-Duarte, E.S., Urbina, J.A., de Souza, W., Vommaro, R.C., 2006. Antiproliferative activities of two novel quinuclidine inhibitors against Toxoplasma gondii tachyzoites in vitro. J. Antimicrob. Chemother. 58, 59–65. https://doi.org/10.1093/jac/dkl180.

Palmie-Peixoto, I.V., Rocha, M.R., Urbina, J.A., de Souza, W., Einicker- Lamas, M., Motta, M.C.M., 2006. Effects of sterol biosynthesis inhibitors on endosymbiont-bearing trypanosomatids. FEMS Microbiol. Lett. 255, 33–42. https://doi.org/10.1111/j.1574-6968.2005.00056.x.

Priest, J.W., Hajduk, S.L., 1994. Developmental regulation of mitochondrial biogenesis in Trypanosoma brucei. J. Bioenerg. Biomembr. 26, 179–191.

Ravera, M., Moreno-Viguri, E., Paucar, R., Perez-Silanes, S., Gabano, E., 2018. Organometallic compounds in the discovery of new agents against kinetoplastid-caused diseases. Eur. J. Med. Chem. 155, 459e48. https://doi.org/10.1016/j.ejmech.2018.05.044.

Rodrigues, J.C.F., Bernardes, C.F., Visbal, G., Urbina, J.A., Vercesi, A.E., de Souza, W., 2007. Sterol methenyl transferase inhibitors alter the ultrastructure and function of the Leishmania amazonensis mitochondrion leading to potent growth inhibition. Protist 158, 447–456. https://doi.org/10.1016/j.protis.2007.05.004.

Rodrigues, C.O., Catisti, R., Uyemura, S.A., Vercesi, A.E., Lira, R., Rodriguez, C., Urbina, J.A., Docampo, R., 2001. The sterol composition of Trypanosoma cruzi changes after growth in different culture media and results in different sensitivity to digitonin permeabilization. J. Eukaryot. Microbiol. 48, 588–594. https://doi.org/10.1111/j.1550-7408.2001.tb00195.x.

Schneider, A., Ochsenreiter, T., 2018. Failure is not an option - mitochondrial genome segregation in trypanosomes. J. Cell Sci. 131https://doi.org/10.1242/jcs.221820. pii: jcs221820.

Silva, J.J., Pavanelli, W.R., Pereira, J.C., Silva, J.S., Franco, D.W., 2009. Experimental chemotherapy against Trypanosoma cruzi infection using ruthenium nitric oxide donors. Antimicrob. Agents Chemother. 53, 4414–4421. https://doi.org/10.1128/AAC.00104-09.

Silva, J.J., Guedes, P.M., Zottis, A., Balliano, T.L., Nascimento Silva, F.O., França Lopes, L.G., Ellena, J., Oliva, G., Andricopulo, A.D., Franco, D.W., Silva, J.S., 2010. Novel ruthenium complexes as potential drugs for Chagas's disease: enzyme inhibition and in vitro/in vivo trypanocidal activity. Br. J. Pharmacol. 160, 260–269. https://doi.org/10.1111/j.1476-5381.2009.00524.x.

Southam, H.M., Butler, J.A., Chapman, J.A., Poole, R.K., 2017. The microbiology of ruthenium complexes. Adv. Microb. Physiol. 71, 1–96. https://doi.org/10.1016/bs.ampbs.2017.03.001.

Stibal, D., Therrien, B., Giannini, F., Paul, L.E.H., Furrer, J., Süss-Fink, G., 2014. Monothiolato bridged dinuclear arene ruthenium complexes: the missing link in the reaction of arene ruthenium dichloride dimers with thiols. Eur. J. Inorg. Chem. 5925–5931. https://doi.org/10.1002/ejic.201402754.

Toueille, M., Saint-Jean, B., Castroviejo, M., Benedetto, J.-P., 2007. The elongation factor 1A: a novel regulator in the DNA replication/repair protein network in wheat cells? PlantPhysiol. Biochem. 45, 113–118. https://doi.org/10.1016/j.plaphy.2007.01.006.

Vercesi, A.E., Docampo, R., 1992. Ca2+ transport by digitonin-permeabilized Leishmania donovani. Effects of Ca2+, pentamidine and WR-6026 on mitochondrial membrane potential in situ. Biochem. J. 284, 463–467. https://doi.org/10.1042/bj2840463.

Verma, N.K., Dey, C.S., 2004. Possible mechanism of miltefosine-mediated death of Leishmania donovani. Antimicrob. Agents Chemother. 48, 3010–3015. https://doi.org/10.1128/AAC.48.8.3010-3015.2004.

Williamson, J., Macadam, R.F., Dixon, H., 1975. Drug-induced lesions in trypanosome fine structure: a guide to modes of trypanocidal action. Biochem. Pharmacol. 24, 147–152. https://doi.org/10.1016/0006-2952(75)90328-7.

Wirtz, E., Leal, S., Ochatt, C., Cross, G.A., 1999. A tightly regulated inducible expression system for conditional gene knock-outs and dominant-negative genetics in Trypanosoma brucei. Mol. Biochem. Parasitol. 99, 89–101. https://doi.org/10.1016/S0166-6851(99)00002-X.

Zimmer, S.L., 2019. Revisiting trypanosome mitochondrial genome mysteries: broader and deeper. Trends Parasitol. 35 (2), 102–104. https://doi.org/10.1016/j.pt.2018.09.006. Feb.